Published OnlineFirst January 8, 2014; DOI: 10.1158/1535-7163.MCT-13-0878

Cancer Biology and Signal Transduction

Molecular Cancer Therapeutics

microRNAs miR-27a and miR-27b Directly Regulate Liver Dihydropyrimidine Dehydrogenase Expression through Two Conserved Binding Sites

Steven M. Offer[1], Gabriel L. Butterfield[1], Calvin R. Jerde[1], Croix C. Fossum[1], Natalie J. Wegner[1], and Robert B. Diasio[1,2]

Abstract

Dihydropyrimidine dehydrogenase (DPD, encoded by *DPYD*) is the rate-limiting enzyme in the uracil catabolic pathway and has a pivotal role in the pharmacokinetics of the commonly prescribed anticancer drug 5-fluorouracil (5-FU). Deficiency of DPD, whether due to inadequate expression or deleterious variants in *DPYD*, has been linked to severe toxic responses to 5-FU. Little is known about the mechanisms governing DPD expression in the liver. In this report, we show increased accumulation of RNA-induced silencing complex (RISC) proteins on *DPYD* mRNA in cells overexpressing the highly homologous microRNAs (miRNA) miR-27a and miR-27b. These miRNAs were shown to repress DPD expression through two conserved recognition sites in *DPYD*. The IC_{50} of 5-FU for HCT116 cells overexpressing miR-27a or miR-27b was 4.4 μmol/L (both), significantly lower than that for cells expressing a nontargeting (scramble) control miRNA (14.3 μmol/L; $P = 3.3 \times 10^{-5}$ and $P = 1.5 \times 10^{-7}$, respectively). Mouse liver DPD enzyme activity was inversely correlated with expression levels of miR-27a ($R^2 = 0.49$; $P = 0.0012$) and miR-27b ($R^2 = 0.29$; $P = 0.022$). A common variant in the hairpin loop region of hsa-mir-27a (rs895819) was also shown to be associated with elevated expression of the miR-27a in a panel of cell lines ($P = 0.029$) and in a transgenic overexpression model ($P = 0.0011$). Furthermore, rs895819 was associated with reduced DPD enzyme activity ($P = 0.028$) in a cohort of 40 healthy volunteers. Taken together, these results suggest that miR-27a and miR-27b expression may be pharmacologically relevant modulators of DPD enzyme function in the liver. Furthermore, our data suggest that rs895819 may be a potential risk allele for 5-FU sensitivity. *Mol Cancer Ther; 13(3); 742–51. ©2014 AACR.*

Introduction

The pyrimidine analog 5-flourouracil (5-FU), and its prodrug capecitabine, are commonly administered for the management of several solid tumors, most notably colorectal cancer. Adverse reactions to 5-FU are relatively frequent, with grade 3 or higher toxicity occurring in up to 34% of recipients (1). Dihydropyrimidine dehydrogenase (DPD) is the rate-limiting enzyme in the uracil catabolic pathway, which is responsible for converting 80% to 90% of administered 5-FU to the inactive metabolite 5-dihydrofluorouracil (2). Certain genetic variations in *DPYD* have been shown to impair DPD enzyme function (3) and significantly increase the risk of fluoropyrimidine toxicity by increasing exposure to 5-FU over time (4). *DPYD* variations are important contributors to 5-FU toxicity risk, although they are thought to only account for approximately 30% of cases of severe toxicity to 5-FU (5).

Intraindividual differences in DPD expression, potentially due to epigenetic factors, have also been suggested to contribute to variable 5-FU sensitivity and variable 5-FU efficacy. 5-FU chemoresistance has been shown to be associated with high tumor expression of DPD in various cancers, including colorectal (6), gastric (7), lung (8), and oral (9) cancers. Strong correlations have been noted between DPD protein expression and enzymatic activity in human lymphocytes (10), and correlations between *DPYD* mRNA expression and DPD activity have been reported in liver specimens (11). However, a number of studies have identified discrepancies between *DPYD* mRNA expression, DPD protein expression, and DPD enzymatic activity [for example (12, 13)], suggesting that DPD expression may be regulated at the posttranscriptional level. Promoter methylation has been proposed as a potential regulatory mechanism for DPD expression (14, 15); however, more recent clinical studies failed to establish an association with toxicity (16). Recent data have suggested that

Authors' Affiliations: [1]Department of Molecular Pharmacology and Experimental Therapeutics and [2]Mayo Clinic Cancer Center, Mayo Clinic, Rochester, Minnesota

S.M. Offer and G.L. Butterfield contributed equally to this article.

Corresponding Author: Robert B. Diasio, Mayo Clinic Cancer Center, 200 1st Street Southwest, Rochester, MN 55905. Phone: 507-266-4997; Fax: 507-538-6670; E-mail: diasio.robert@mayo.edu

doi: 10.1158/1535-7163.MCT-13-0878

Published OnlineFirst January 8, 2014; DOI: 10.1158/1535-7163.MCT-13-0878

microRNAs (miRNA) may posttranscriptionally regulate DPD expression in lung tumors, (17) although the contributions to 5-FU sensitivity and resistance have not been evaluated.

The objectives of the present study were to determine the physiologic relevance of miR-27a- and miR-27b-mediated regulation of DPD to 5-FU toxicity and resistance. This study additionally investigated the functional impact of the hsa-mir-27a hairpin region single-nucleotide polymorphism (SNP) rs895819 on expression of mature miR-27a and, consequently, DPD enzymatic activity in human circulating cells. On the basis of computational predictions, we hypothesized that miR-27a and miR-27b posttranscriptionally repressed DPD through two recognition sequences located directly upstream and downstream of the *DPYD* termination codon. The results presented in this article provide direct physiologic evidence that miR-27a and miR-27b are important contributors to cellular sensitivity to 5-FU.

Materials and Methods

Cells

Low-passage HEK293T/c17 (culture CRL-11268), HCT116 (culture CCL-247), and HT-29 (culture HTB-38) cells were obtained from the American Type Culture Collection (ATCC) and maintained at 37°C in a humidified incubator with an atmosphere of 5% CO_2. Cells were cultured using Dulbecco's Modified Eagle Medium (Mediatech) supplemented with 10% FBS (Denville Scientific), 100 U/mL penicillin (Mediatech), and 100 μg/mL streptomycin (Mediatech). Lymphoblastoid cell lines from unrelated individuals were obtained from the Coriell Institute for Medical Research (Camden, NJ) and were maintained in RPMI-1640 medium (Mediatech) supplemented with 10% FBS, 100 U/mL penicillin, and 100 μg/mL streptomycin. Cell identities of all lines were confirmed and monitored as previously reported (3). Aliquots of low-passage cells were cryopreserved within 2 weeks of receipt. Cells were cultured for no more than 10 total passages or 2 months. All cell lines were periodically monitored for mycoplasma using Hoechst staining (Sigma-Aldrich). Culture identity and health were monitored by microscopy and by comparing the population doubling times with baseline values determined at the time of receipt. Additional authentication of cell lines beyond that described above was not performed.

Vector construction

To generate miRNA expression vectors, annealed oligonucleotides (Integrated DNA Technologies) were cloned into the pLKO.1-TRC vector (18), which was obtained from Addgene (plasmid #8453). Control vectors pCMV-GFP (plasmid 11153; ref. 19) and pLKO.1-scramble (plasmid 17920; ref. 20), and lentiviral packaging vectors pMD2.G (plasmid 12259) and psPAX (plasmid 12260), were obtained from Addgene. Plasmid sequences were confirmed at the Mayo Clinic Advanced Genomics Technology Center (Rochester, MN).

Lentiviral production

Lentiviral particles were produced by cotransfection of HEK293T/c17 cells with expression and packaging vectors using TransIT-LT1 (Mirus Bio) at the ratios recommended by Addgene. Twenty-four hours following transfection, media were removed, cells were rinsed with PBS, and fresh media added back to plates. Virus-containing supernatants were collected at 48 and 72 hours after transfection and pooled. To remove cellular debris, supernatants were centrifuged at 600 $\times g$ and passed through a 0.45-μm PES membrane filter (EMD Millipore). All transductions were conducted in the presence of 8 μg/mL final concentration polybrene (EMD Millipore). Transduction with viral supernatants for pCMV-GFP, prepared in parallel with experimental samples, was used to assess transduction efficiency.

Western blotting

Protein lysates were separated on a 10% SDS-PAGE gel and transferred to polyvinylidene difluoride (PVDF)-FL membrane (EMD Millipore). Membranes were blocked using Odyssey blocking buffer (LI-COR Biosciences). Blots were probed with primary antibodies against DPD and α-tubulin (both AbCam) and subsequent secondary IRDye800-conjugated goat anti-mouse and IRDye680-conjugated goat anti-rabbit (both LI-COR Biosciences). Blots were scanned and band intensities quantified using the Image Studio 3.1 and LI-COR Odyssey Infrared Imaging System according to manufacturer's instructions.

Measurement of *DPYD* gene expression

Total RNA was extracted using TRizol and the NucleoSpin miRNA purification kit. Reverse transcription reactions were completed using Transcriptor Reverse Transcriptase with oligo-d(T) primers, according to manufacturer's directions. Quantitative PCR was carried out using PrimeTime qPCR Primer/Probe Assays (Integrated DNA Technologies) in LightCycler 480 Probes Master enzyme mix (Roche Applied Science). Human *DPYD* and *GAPDH* were amplified and detected using PrimeTime assay numbers Hs.PT.56a.40723155 and Hs.PT.39a.22214836, respectively. Amplification efficiencies for both assays were greater than 95% (data not shown). As such, the $2^{-\Delta\Delta C_T}$ method, in which $\Delta\Delta C_T = [C_{T\ DPYD} - C_{T\ GAPDH}]_{sample} - [C_{T\ DPYD} - C_{T\ GAPDH}]_{scr}$, was used to measure *DPYD* expression for cells overexpressing miR-27a and miR-27b ("sample" in the above equation) normalized to expression for cells overexpressing the nontargeting control ("scr" in the above equation) at each time point assayed. Methods and reagents used to measure gene expression in mouse tissues are detailed in the relevant subsection below.

Cell viability assays

Cell viability in the presence of 5-FU was measured in HCT116 cells following transduction of lentiviral particles using CellTiter-Blue (Promega) as previously reported (3).

Published OnlineFirst January 8, 2014; DOI: 10.1158/1535-7163.MCT-13-0878

Luciferase reporter system

HCT116 RNA was reverse transcribed using the Transcriptor High Fidelity cDNA Synthesis Kit (Roche Applied Science) using oligo-d(T) primers. The 3′ 56 nucleotides of the open reading frame (ORF) and the 3′ untranslated region (3′-UTR) of *DPYD* were amplified by PCR (Phusion High-Fidelity DNA Polymerase; New England Biolabs) using primers 5′-CAACACCTTATGAACCAAAGAGAGGC-3′ and 5′-ATGCTTTATGATATTTTATTTG-3′ and cloned into the pTK-Gluc vector (New England Biolabs). Mutations were introduced into the predicted miRNA seed-binding sites using the Phusion Site-Directed Mutagenesis Kit (New England Biolabs). Independent clonal cell lines stably expressing each of the reporter constructs were selected using G418 (Mediatech), following transfection of linearized plasmid. miRNA mimics and inhibitors were obtained from Qiagen and transfected using HiPerFect (Qiagen) as per manufacturer's instructions. AllStars Hs Cell Death siRNA (Qiagen) was used as a transfection control and to establish residual luciferase activity at time of reading. Luciferase levels were measured after 48 hours using the BioLux Gaussia Luciferase Flex Assay Kit (New England Biolabs). Luciferase activity is reported relative to that for the scramble control. *P* values were determined using a two-tailed unpaired Student *t* test.

Mouse lines and tissue preparation

Remnant liver tissues from FVB/NTac female mice (lines obtained from Taconic) that were older than 8 weeks were kindly provided by Dr. Paul F. Lambert, at the University of Wisconsin–Madison (Madison, WI). Tissue collection was conducted in accordance with protocols approved by the Institutional Animal Care and Use Committee (IACUC) of the University of Wisconsin. Following resection from mice, livers were immediately snap frozen and stored at −80°C until use. For enzyme activity quantitation, specimens were lysed using a Bullet Blender Storm (Next Advance) with an equivalent tissue volume of 0.1-mm diameter glass beads in buffer consisting of 35 mmol/L potassium phosphate at pH 7.4, 2.5 mmol/L $MgCl_2$, 0.035% 2-mercaptoethanol, and cOmplete EDTA-free protease inhibitor cocktail (Roche Applied Science). Lysates were cleared by centrifugation and total protein concentration was determined using the Pierce 660 nm Protein Assay (Thermo Fisher Scientific). DPD enzyme activity was measured using the high-performance liquid chromatography (HPLC)–based assay previously reported by our laboratory (3).

For total RNA isolation, liver tissues were lysed in TRizol (Life Technologies) with an equivalent tissue volume of 0.1-mm diameter glass beads using the Bullet Blender Storm. Total RNA was purified using the NucleoSpin miRNA purification kit (MACHEREY-NAGEL), and reverse transcription reactions were performed using the Universal cDNA Synthesis Kit II (Exiqon). Quantitative PCR was carried out using TaqMan Gene Expression Assays (Life Technologies) primer and probes in LightCycler 480 Probes Master enzyme mix (Roche Applied Science). Mouse *DPYD* and *GAPDH* were amplified and detected using assay numbers Mm00468111_m1 and Mm99999915_g1, respectively, and calculation of normalized relative *DPYD* expression was performed as described for human *DPYD* above. miRNA expression was measured for mouse tissues similarly as for cell lines as described below.

miRNA expression

Total RNA from cell lines was harvested using TRizol followed by purification using the NucleoSpin miRNA purification kit. RNA was treated using Ambion TURBO DNase Treatment and Removal reagents (Life Technologies) as per manufacturer's instructions. RNA from mice was purified as described above. Reverse transcription reactions were performed using the Universal cDNA Synthesis Kit II (Exiqon). miRNA expression was assayed by quantitative PCR using locked nucleic acid (LNA)–based primers specific to each miRNA. Primers were ordered from Exiqon to amplify miR-27a (product number 204764), miR-27b (product number 205915), and RNU5G (product number 203908). Reactions were carried out using LightCycler 480 SYBR Green I Master on a LightCycler 480 (Roche Applied Science) using cycling parameters recommended by manufacturer. Amplification products were confirmed by melt curve analysis. Relative expression of miR-27a and miR-27b relative to RNU5G was determined using the $2^{-\Delta\Delta C_T}$ method as described above.

RNA-induced silencing complex immunoprecipitation

The RNA-induced silencing complex (RISC) immunoprecipitation (IP) protocol was adapted from that of Keene and colleagues (21). Briefly, HCT116 cells were transduced as described above and lysed in polysome lysis buffer (21). A mixture of Protein A and Protein G PureProteome Magnetic Beads (EMD Millipore) were precoated with anti-pan AGO antibody (clone 2A8; EMD Millipore) and subsequently mixed with precleared lysate. Following washes, beads were resuspended in NT2 buffer (21) supplemented with Proteinase K (Roche Applied Science). Total RNA was extracted using TRizol and the NucleoSpin miRNA purification kit. Reverse transcription reactions were completed using Transcriptor Reverse Transcriptase using a mixture of oligo-d(T) and random hexamer primers, according to manufacturer's directions. Quantitative PCR for *DPYD* was carried out using PrimeTime qPCR Primer/Probe Assay Hs.PT.56a.40723155 (Integrated DNA Technologies) in LightCycler 480 Probes Master enzyme mix.

Human volunteer study

DNA from 53 African American volunteers collected previously at University of Alabama at Birmingham was genotyped for rs895819 using a TaqMan genotyping assay available from Life Technologies. *DPYD* genotypes and

Published OnlineFirst January 8, 2014; DOI: 10.1158/1535-7163.MCT-13-0878

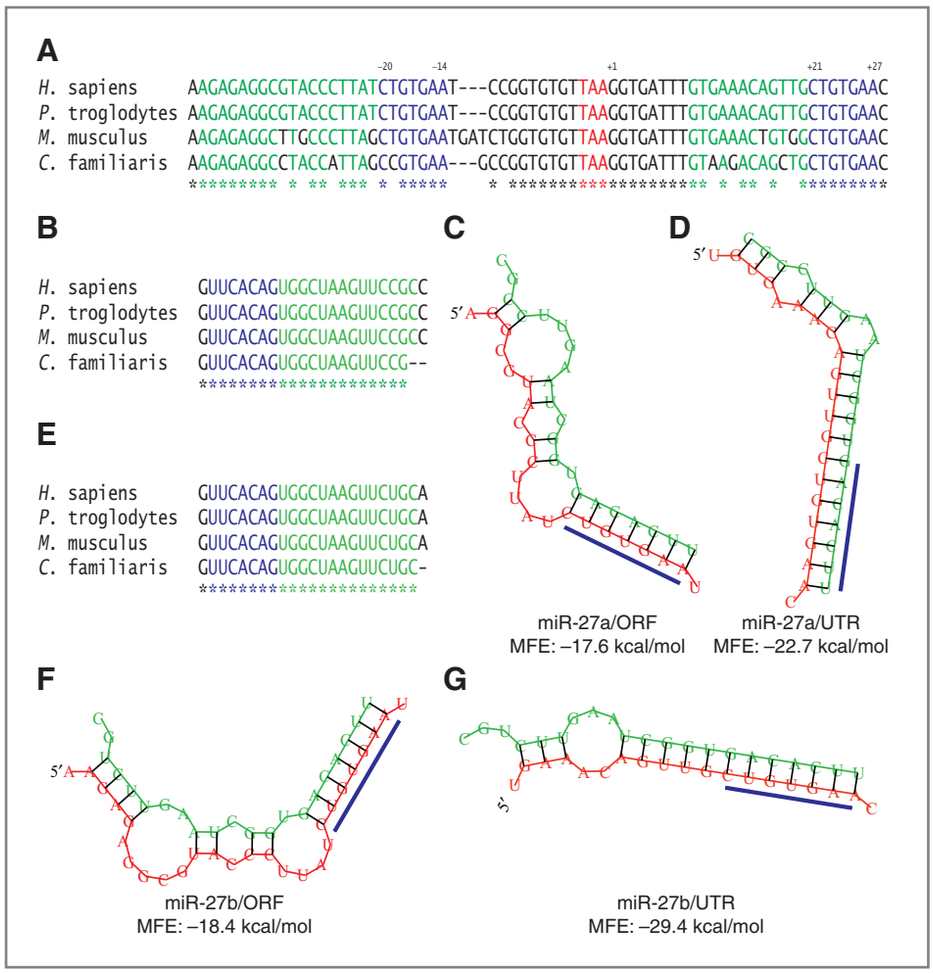

Figure 1. Identification of candidate miR-27a and miR-27b binding sites in the *DPYD* gene. A, alignment of mammalian *DPYD* (NM_000110) sequences for *Homo sapiens*, *Pan troglodytes*, *Mus musculus*, and *Canis familiaris*. Red letters, stop codon; blue letters, predicted seed-binding sequences; green letters, predicted flanking miRNA-binding sequences; *, fully conserved nucleotides. The position of the predicted seed-binding regions is reported above the alignment relative to the first nucleotide of the 3′ UTR with coordinates reported relative to the *Homo sapiens* sequence. B, conservation of mature miR-27a sequences. The MFE structures of miR-27a complexed to the predicted ORF (C) and UTR (D) binding sites of *Homo sapiens DPYD* were predicted using RNAhybrid (25). E, sequence conservation of mature miR-27b. Predicted structures of miR-27b bound to the ORF (F) and UTR (G) binding sites.

DPD enzyme activity have been previously reported for all individuals used in this study (22), which was approved by the Institutional Review Boards of the University of Alabama at Birmingham (IRB# F020610007 and X000830002) and subsequently at Mayo Clinic (IRB# 09-007080). Inclusion in the present study was contingent on the availability of adequate DNA for genotyping and the lack of known variants associated with DPD deficiency, including *DPYD*: IVS14+1G>A (rs3918290), p.I560S (rs55886062), p.D949V (rs67376798), or p.Y186C (rs115232898). Statistical tests were performed using PLINK version 1.07 (23) and the R Environment for Statistical Computing version 3.0.1 (R Foundation for Statistical Computing).

Bioinformatics

Potential miRNA binding sites were predicted using the software package PicTar (24). RNA:miRNA duplex structures were predicted, and minimum free energy (MFE) values were calculated using the RNAhybrid software program (25). The RNAfold software program, as implemented in the Vienna RNA Package version 2.0 (26), was used to predict MFE and centroid (weighted average of possible conformations) pre-miRNA hairpin structures.

Statistical tests

All data analyses and transformations were performed using JMP version 9.0.3 (SAS Institute Inc.), unless otherwise noted. Additional tests and software algorithms used are described in relevant sections above.

Results

In silico modeling predicts two binding sites for miR-27a and miR-27b in *DPYD*

miRNA target specificity is largely determined by the approximately 7-nucleotide region at the 5′ end of the miRNA, termed the seed region. Candidate miRNA target sites in the 3′ UTR of *DPYD* (NM_000110) were predicted using PicTar (24). A conserved seed-region binding site for miR-27a and miR-27b was detected in the 3′ UTR, located 21 to 27 nucleotides downstream of the stop codon (Fig. 1A). A manual search of the mRNA revealed an additional conserved seed-region site located 14 to 20 nucleotides upstream of the 3′ UTR in the ORF. The sequence of miR-27a is highly conserved in mammals (Fig. 1B) and has a calculated MFE of −17.6 kcal/mol when bound to the ORF binding site (Fig. 1C) and an MFE

Published OnlineFirst January 8, 2014; DOI: 10.1158/1535-7163.MCT-13-0878

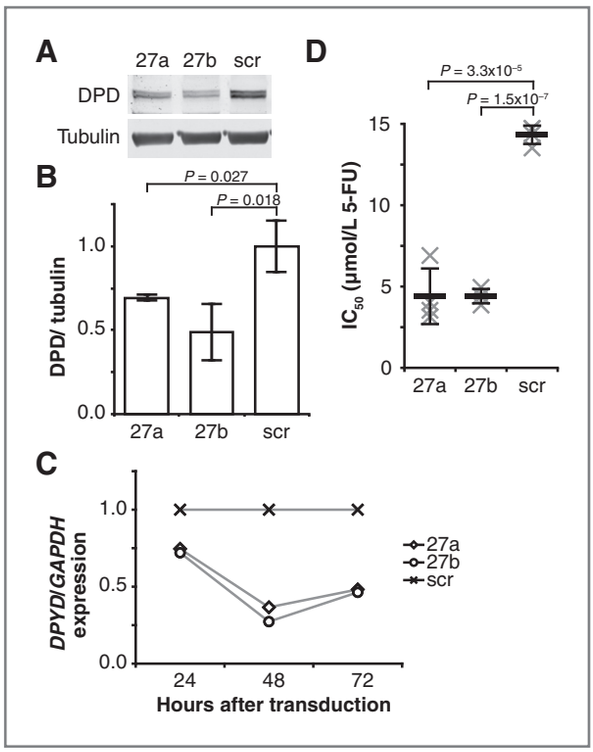

Figure 2. miR-27a and miR-27b downregulate DPD expression and sensitize cells to 5-FU. A, DPD and α-tubulin expression were measured following transduction of HCT116 cells with lentiviral particles encoding miR-27a (27a), miR-27b (27b), or a nontargeting control miRNA (scr). A representative blot is presented. B, mean DPD protein expression ± SD for three independent replicate experiments is presented. C, expression of *DPYD* mRNA relative to *GAPDH* was measured at the indicated time points by quantitative RT-PCR. Transduction of HCT116 cells was performed as in Figure 2A. Results are presented relative to nontargeting (scr) control. A representative experiment is presented. D, the mean inhibitory concentration (IC_{50}) for 5-FU was determined for HCT116 cells transduced as in Figure 2A. Results for each of four individual biologic replicate are presented as an "x." Horizontal bars, mean IC_{50} values; whiskers, SDs.

of −22.7 kcal/mol when bound to the UTR binding site (Fig. 1D). miR-27b is likewise highly conserved (Fig. 1E), and shows a favorable calculated MFE when bound to the ORF (−18.4 kcal/mol; Fig. 1F) and the UTR (−29.4 kcal/mol; Fig. 1G) predicted sites.

Endogenous DPD expression is reduced by miR-27a and miR-27b overexpression

DPD expression was measured in HCT116 colorectal carcinoma cells after transduction with lentiviral particles encoding miR-27a, miR-27b, or a nontargeting (scramble) control. Seventy-two hours following transduction, we noted robust reductions of endogenous DPD expression for cells overexpressing either miR-27a or miR-27b relative to the nontarget control (Fig. 2A). Quantitation of pooled results from replicate experiments showed that cells overexpressing miR-27a had a 31% reduction in DPD expression compared with control ($P = 0.027$), and that DPD expression was repressed by 51% in miR-27b–overexpressing cells ($P = 0.018$, Fig. 2B). Similar results were noted when experiments were repeated using HT29 colorectal adenocarcinoma cells (data not shown). This reduction in protein level was accompanied by reduced mRNA expression (Fig. 2C), suggesting that repression of expression occurs, at least in part, through targeted degradation of *DPYD*.

miR-27a and miR-27b expression sensitizes cells to 5-FU

To determine whether the level of DPD repression was adequate to affect cellular sensitivity to 5-FU, the IC_{50} for the drug was determined in HCT116 cells overexpressing miR-27a, miR-27b, or a nontargeting (scramble) control (Fig. 2D). The IC_{50} for 5-FU in cells expressing miR-27a or miR-27b was 4.4 μmol/L and 4.4 μmol/L, significantly lower than that for the nontargeting control, 14.3 μmol/L ($P = 3.3 \times 10^{-5}$ and $P = 1.5 \times 10^{-7}$, respectively).

Argonaute-mediated interaction between *DPYD* and miR-27a/miR-27b

To determine whether miR-27a and miR-27b repressed DPD expression via recruitment of RISC components to the *DPYD* transcript, lysates from cells overexpessing miR-27a, miR-27b, or the nontargeting (scramble) control were immunoprecipitated using anti-pan AGO antibodies. The relative amounts of RISC-associated *DPYD* were measured using quantitative real-time (RT)-PCR. A schematic of the RISC-IP procedure is presented in Fig. 3A.

Cells overexpressing miR-27a showed a 2.2-fold increase in RISC-associated *DPYD*, relative to cells expressing the nontargeting control ($P = 0.0098$; Fig. 3B); a 3.0-fold increase over control was noted for cells overexpressing miR-27b ($P = 0.032$). Nonspecific antibody-independent binding of *DPYD* to Protein A/G substrate was undetectable, and total RNA yields were <0.4% of those from experimental samples (data not shown). These data suggest that miR-27a and miR-27b can mediate the targeting of AGO-containing RISC complexes to *DPYD* to regulate expression of DPD.

Both putative binding sites are targets of miR-27a and miR-27b

To determine which of the predicted binding sites are functional targets for miR-27a and miR-27b, we generated luciferase reporter constructs containing the 3′ UTR of *DPYD* with an additional 56 bases of upstream ORF sequence, which contained the second predicted binding site (Fig. 4A). To confirm specificity for the identified binding sites, mutations were introduced into the predicted ORF-binding site, the predicted UTR-binding site, and both binding sites (Fig. 4B). Independent clonal HCT116 cell lines stably expressing each of the luciferase reporter constructs were selected and transfected with RNA mimics of miR-27a, miR-27b, or a nontargeting control miRNA with no homology to known protein-coding genes. Mutation of both binding sites led to a significant increase in luciferase activity following transfection with

Published OnlineFirst January 8, 2014; DOI: 10.1158/1535-7163.MCT-13-0878

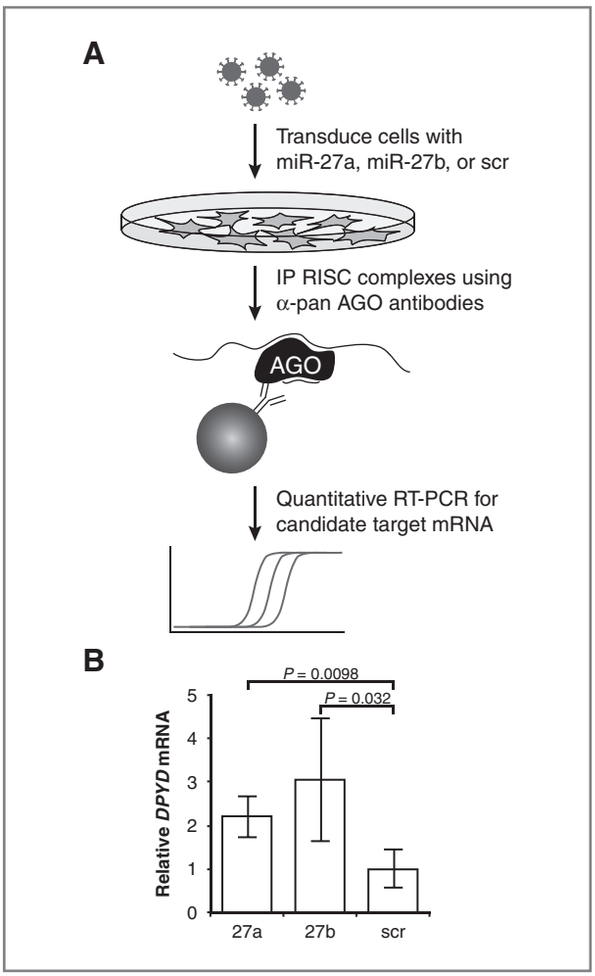

Figure 3. Increased association of RISC proteins with *DPYD* in cells overexpressing miR-27a and miR-27b. A, the schematic of the RNA immunoprecipitation (IP) protocol is presented. B, relative *DPYD* mRNA in immunoprecipitates was measured using quantitative RT-PCR for HCT116 cells transduced with lentiviral particles encoding miR-27a (27a), miR-27b (27b), or a nontargeting control miRNA (scr). Four independent replicate experiments were performed; data were normalized between experiments by dividing by the mean relative expression within a given replicate.

miR-27a mimics ($P = 1.9 \times 10^{-4}$, Fig. 4C), suggesting that the sites may be targets of miR-27a–mediated repression. Mutations at either single binding site also caused a significant, but less severe, increase in luciferase activity following miR-27a transfection ($P = 0.048$ and $P = 0.0051$). Compared with cells expressing the reporter with both sites mutated, those with single-site mutations had significantly lower luciferase activity ($P = 0.0095$ and $P = 0.035$). Similar trends were noted for cells transfected with miR-27b (Fig. 4C), in which mutation of both binding sites significantly increased luciferase activity ($P = 1.6 \times 10^{-5}$), and mutation of either single site resulted in an intermediate increase in activity ($P = 0.026$ and $P = 0.0030$) that was significantly lower than the double-site mutation ($P = 0.0039$ and $P = 0.0060$). No significant differences in luciferase expression were noted between the single-site mutations following transfection with either miRNA, suggesting that both sites may participate in repression.

Correlation between DPD activity and miRNA expression in liver

Following administration, the majority of 5-FU catabolism occurs in the liver. To determine if miR-27a and miR-27b levels correlated with DPD function *ex vivo*, liver RNA and protein were purified from 18 mice. DPD protein activity was assayed for each protein lysate by measuring the reduction of radiolabeled 5-FU to 5,6-dihydrofluorouracil (DHFU), and expression of miR-27a, miR-27b, and

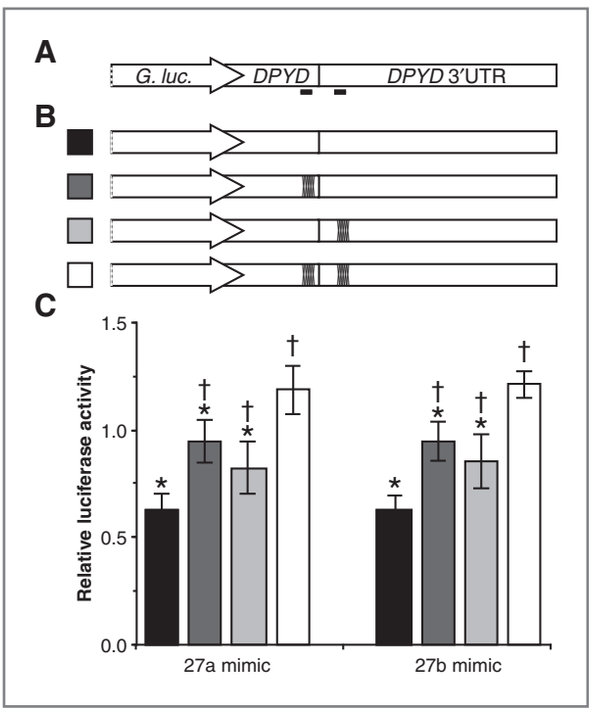

Figure 4. miR-27a and miR-27b recognize both predicted target sites in *DPYD*. A, the 3′ UTR and 56 nucleotides of upstream coding ORF sequence of *DPYD* were cloned into expression vectors directly downstream of the *Gaussia luciferase* gene. Solid black bars, locations of the predicted miR-27a and miR-27b binding sites. B, expression vectors harboring mutations in the predicted miRNA binding sites were generated. Dark marks on the diagram indicate that mutations were introduced into that particular site. Stable clonal HCT116 cell lines expressing each of the indicated vectors were generated. Three clonal lines each were generated expressing the single-site mutations (dark gray and light gray). Four clonal lines were generated to express the unmutated construct (black) and the double-site disruptions (white). C, relative luciferase activity was determined following transfection with RNA mimics of miR-27a, miR-27b, and a nontargeting control miRNA. Results were normalized to the nontargeting control. Each cell line was transfected and relative luciferase activity was measured in triplicate. The mean relative luciferase activity of clonal lines is presented ± SD. *P* values were calculated using the two-tailed unpaired Student *t* test, assuming normal distribution. Constructs showing significantly lower luciferase activity compared with clones expressing the double-mutations construct ($P < 0.05$) are indicated with an asterisk; those showing significantly higher luciferase activity than clones expressing the unmutated construct ($P < 0.05$) are indicated with a dagger.

Published OnlineFirst January 8, 2014; DOI: 10.1158/1535-7163.MCT-13-0878

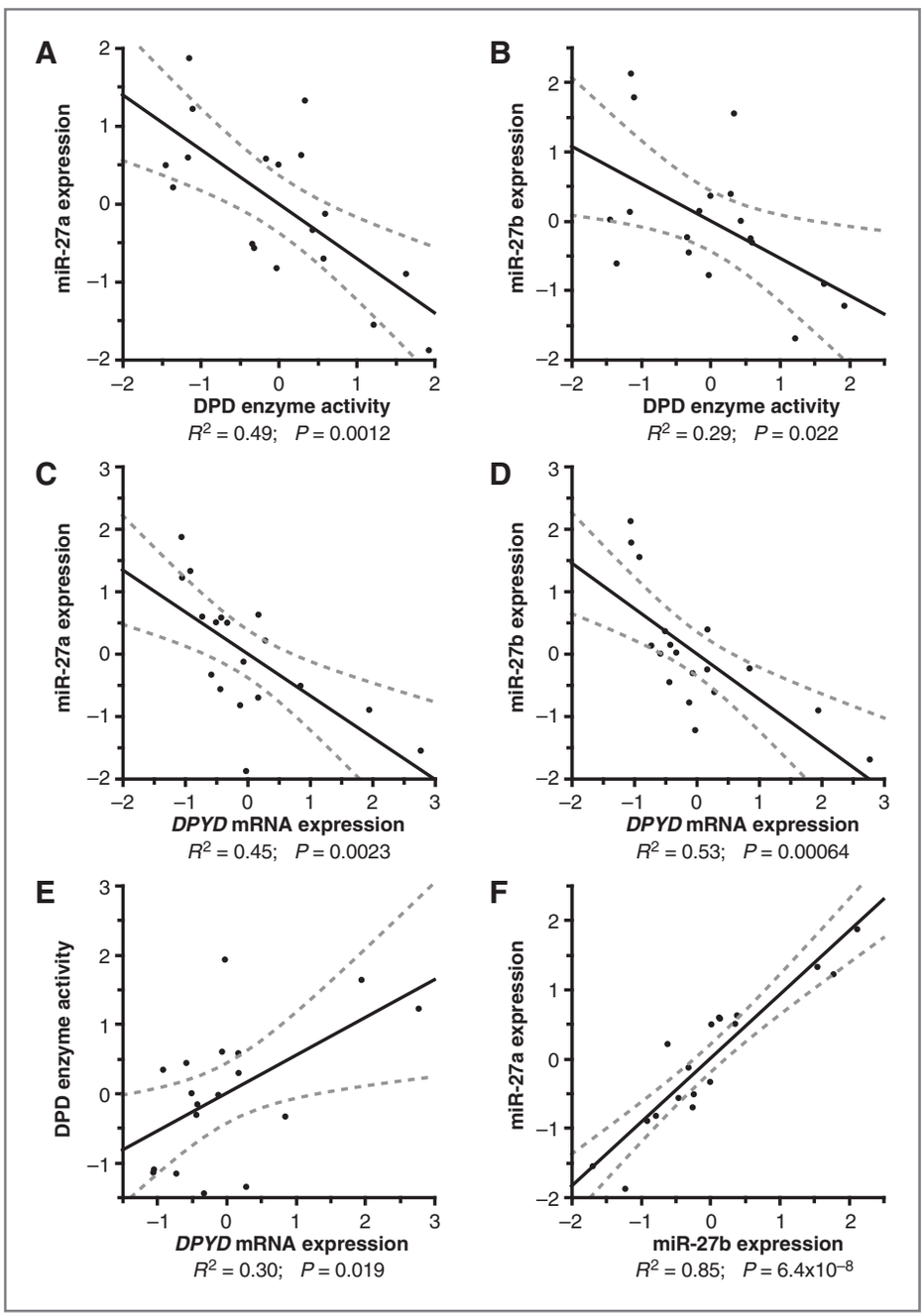

Figure 5. miR-27a/miR-27b expression correlates with reduced DPD enzyme activity and reduced *DPYD* expression in liver tissue. Liver specimens were obtained from 18 euthanized mice and were immediately flash frozen in liquid nitrogen. Expression of *DPYD*, miR-27a, and miR-27b were determined by quantitative RT-PCR. DPD enzyme activity was inversely correlated with both miR-27a (A) and miR-27b (B) expression. *DPYD* expression was also inversely correlated with both miR-27a (C) and miR-27b (D) expression. DPD enzyme activity and *DPYD* expression were positively correlated (E); miR-27a and miR-27b expressions were also positively correlated (F). miR-27a and miR-27b expression values are reported relative to *RNU5G*. *DPYD* expression is reported relative to *GAPDH*. For all calculations, values were normalized to the mean and are presented as SDs from the mean for the analyte reported on each axis (*Z*-score normalization). Solid black line, linear regression of the data; dotted gray line, 95% confidence interval of the regressed line.

DPYD were measured using quantitative RT-PCR. DPD enzyme activity was negatively correlated with expression of miR-27a ($P = 0.0012$; Fig. 5A) and miR-27b ($P = 0.022$; Fig. 5B). Negative correlations with *DPYD* expression were also noted for miR-27a ($P = 0.0023$; Fig. 5C) and miR-27b ($P = 6.4 \times 10^{-4}$; Fig. 5D). As expected, positive correlations were noted between *DPYD* expression and DPD activity ($P = 0.019$; Fig. 5E) and between miR-27a and miR-27b expression ($P = 6.4 \times 10^{-8}$, Fig. 5F). These results provide evidence that miR-27a and miR-27b regulate liver DPD and are involved in 5-FU catabolism *in vivo*.

Effect of rs895819 on miR-27a expression

The rs895819 polymorphism, located within the coding region for the hsa-mir-27a hairpin, is relatively common with a global minor allele frequency of 35%, as estimated using 1000 Genomes data (27). To determine the impact of this SNP on the stability of the hairpin structure, we modeled the MFE and centroid structures (weighted average of possible structural conformations) for hsa-mir-27a with and without the rs895819 variant using RNAfold (26). The larger hairpin structure shown on the left-hand side of Fig. 6A contains the rs895819 variant,

Published OnlineFirst January 8, 2014; DOI: 10.1158/1535-7163.MCT-13-0878

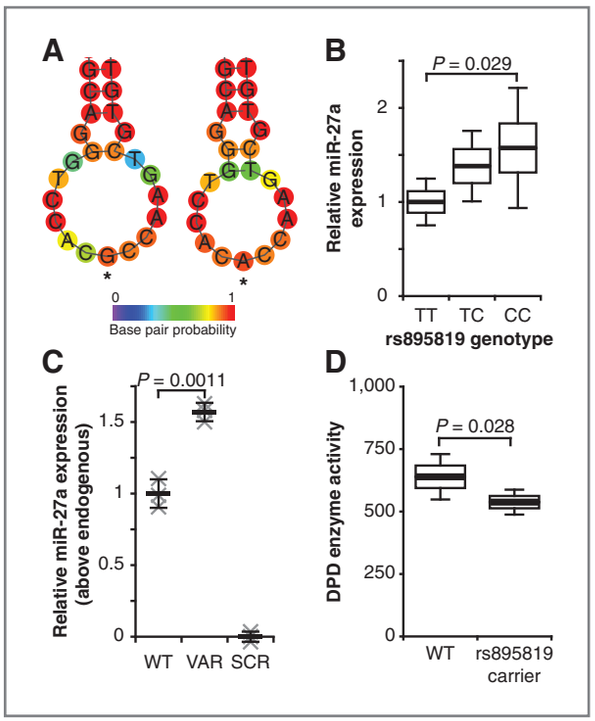

Figure 6. The hsa-mir-27a hairpin SNP rs895819 leads to increased expression of mature miR-27a. A, hsa-mir-27a centroid structures corresponding to the T and variant C alleles of rs895819 (A and G in the hairpin structures were modeled using RNAfold; ref. 26). A color scale representing the probability of base pairing for each residue is presented. B, expression of mature miR-27a was determined by quantitative RT-PCR for 94 lymphoblastoid cell lines that were genotyped for rs895819. Results are reported relative to the control RNU5G. Horizontal bars, mean expression; boxes, SEM; error bars, 95% confidence intervals. C, expression vectors encoding wild-type hsa-mir-27a (T allele, WT), rs895819 (C allele, VAR), and a nontargeting control miRNA (SCR) were transfected into HEK293T/c17 cells and expression of mature miR-27a was measured by quantitative RT-PCR. Three independent biologic replicates were performed. Data for each replicate were normalized using the *Z*-score method, and pooled data were rescaled relative to SCR and WT. D, healthy volunteers for whom DPD enzyme function had been previously quantified (22) were genotyped for the rs895819 variant. DPD enzyme activity (presented as pmol 5-FU reduced per min per mg of total protein) following correction for covariates (age, sex, and *DPYD*-p.C29R status) is presented for noncarriers (WT) and carriers of rs895819. Mean, SE, and 95% confidence intervals are presented as in B. *P* values for all experiments were calculated using the two-tailed Student *t* test.

which results in a loop region that is two bases larger than the "wildtype" hairpin shown on the right-hand side. Larger hairpin loop regions of many miRNA precursors, including hsa-mir-27a, have been previously shown to be more effectively processed, prompting our hypothesis that expression of miR-27a would be higher in the presence of rs895819 due to more effective miRNA maturation (28). To test this hypothesis, we measured miR-27a expression in lymphoblastoid cell lines that had been genotyped for rs895819 (Fig. 6B). Cells homozygous for the SNP (C allele) had approximately 50% higher miR-27a expression compared with those homozygous for the wild-type T allele ($P = 0.029$). Intermediate expression was noted for heterozygous cell lines.

To confirm that the noted expression differences were not an artifact of the varied genetic background of the lymphoblastoid lines, expression constructs encoding the wild-type and variant alleles were expressed in HEK293T/c17 cells. miR-27a expression was 57% higher in cells expressing the variant construct encoding the G allele (corresponding to the C genotype for rs895819) compared with those expressing the wild-type A allele ($P = 0.0011$; Fig. 6C).

To determine whether the effect of rs895819 on miR-27a expression was adequate to affect DPD enzyme activity in carriers of the SNP, we genotyped for the variant in a cohort of individuals in which we previously measured DPD enzyme activity in peripheral blood mononuclear cells (22). A multivariate analysis using a general linear model was used to test for association between rs895819 and altered DPD enzyme activity. Age, sex, and the *DPYD* SNP p.C29R (rs1801265), which previously showed evidence for contributing to increased DPD enzyme activity in circulating cells (22), were treated as covariates. A dominant model for rs895819, in which both heterozygous and homozygous carriers of the variant were grouped, was assumed for these analyses. Following correction for covariates, carriers of rs895819 showed significantly less enzyme activity than noncarriers ($P = 0.028$, Fig. 6D). This finding suggests that rs895819 may contribute to 5-FU response.

Discussion

As the rate-limiting enzyme of the uracil catabolic pathway, DPD plays a critical role in determining the pharmacokinetics of 5-FU. Other than genetic variants in *DPYD*, the mechanisms that regulate DPD enzyme activity in the liver, and by extension 5-FU cytotoxicity, are poorly understood. In this study, we addressed this limitation and provide physiologically relevant evidence that DPD is posttranscriptionally controlled by two highly homologous miRNAs, miR-27a and miR-27b.

Previous reports have suggested that miR-27a may contribute to 5-FU resistance in tumors, potentially through indirect regulation of the drug efflux protein multidrug resistance protein 1 (MDR1, encoded by *ABCB1*; refs. 29–31); however, the role of MDR1 in 5-FU transport is unclear (32). In the present article, we provide evidence that AGO proteins, catalytic components of RISC, accumulate in greater numbers on *DPYD* mRNA in cells that overexpress miR-27a and miR-27b (Fig. 3), leading to repression of DPD (Fig. 2A and B) and increased sensitivity to 5-FU (Fig. 2D). These data are supported by luciferase reporter studies presented in Fig. 4. Deletion of either predicted miR-27a/miR-27b recognition site in *DPYD* significantly increased luciferase expression, suggesting that both sites may be targets of RISC-mediated repression (Fig. 4C). Overall, these data suggest that *DPYD* is a direct downstream target of miR-27a and miR-27b, and that expression levels of either miRNA may, thus, directly affect tumor response to

Published OnlineFirst January 8, 2014; DOI: 10.1158/1535-7163.MCT-13-0878

5-FU. Additional studies are needed to clarify the contributions to 5-FU sensitivity of other pathways downstream of miR-27a and miR-27b.

As the primary site of 5-FU inactivation, 80% to 90% of administered 5-FU is inactivated by DPD in the liver (2). As such, alteration in liver DPD activity can have profound effects on 5-FU pharmacokinetics, which could potentially lead to decreased drug efficacy due to elevated catabolism (high DPD expression) or clinical toxicity due to impaired catabolism (low DPD expression). In the present study, we provide evidence that liver DPD expression may be regulated in part by miR-27a and miR-27b (Fig. 5A and B). These correlations are consistent with those previously reported for miR-27a and 5-FU sensitivity in cellular models of hepatocellular carcinoma (31). In our study, inverse correlations were also noted between *DPYD* mRNA expression and miR-27a/miR-27b expression (Fig. 5C and D), and *DPYD* mRNA expression was reduced following overexpression of either miR-27a or miR-27b (Fig. 2C). These data are consistent with miR-27a/miR-27b targeting RISC proteins to *DPYD*, leading to mRNA degradation as a means to repress DPD expression (33).

Finally, we present evidence that a variant within the hsa-mir-27a hairpin-coding region (rs895819) can alter miR-27a expression and subsequently DPD enzyme levels (Fig. 6). Studies of the relevance of rs895819 to various cancers have yielded unclear, and at times conflicting, results. The variant C allele has been shown to be protective against certain types of breast cancer (34–36), to be both a risk (37) and protective (38) allele in gastric cancer, and unassociated with risk in colorectal cancer (39). Although the variant was originally hypothesized to impair maturation of miR-27a (34), it was later shown to correlate with increased expression (37). This result is consistent with the increase in miR-27a expression we noted in both lymphoblastoid lines (Fig. 6B) and by direct evaluation of function using an isogenic system of expression (Fig. 6C). We additionally showed that DPD activity was significantly lower in rs895819 carriers than in noncarriers (Fig. 6D). Further studies are underway to determine whether the reduction (and the SNP) associates with clinical 5-FU toxicity.

Overall, these findings demonstrate that *DPYD* may be a direct functional target of RISC-mediated repression by miR-27a and miR-27b. The results presented in this article provide evidence that regulation of DPD by miR-27a/miR-27b may be physiologically relevant to both tumor resistance and clinical toxicity to 5-FU–based chemotherapy.

Disclosure of Potential Conflicts of Interest

No potential conflicts of interest were disclosed.

Authors' Contributions

Conception and design: S.M. Offer, G.L. Butterfield
Development of methodology: S.M. Offer, G.L. Butterfield, C.R. Jerde, N.J. Wegner
Acquisition of data (provided animals, acquired and managed patients, provided facilities, etc.): S.M. Offer, G.L. Butterfield, C.R. Jerde, C.C. Fossum, N.J. Wegner
Analysis and interpretation of data (e.g., statistical analysis, biostatistics, computational analysis): S.M. Offer, G.L. Butterfield, C.R. Jerde, N.J. Wegner, R.B. Diasio
Writing, review, and/or revision of the manuscript: S.M. Offer, G.L. Butterfield, C.R. Jerde, R.B. Diasio
Administrative, technical, or material support (i.e., reporting or organizing data, constructing databases): C.R. Jerde
Study supervision: S.M. Offer, R.B. Diasio

Acknowledgments

The authors thank Dr. Paul Lambert and Amy Liem of the McArdle Laboratory for Cancer Research at the University of Wisconsin–Madison for providing mouse liver samples, and David Root (Broad Institute of Harvard and MIT, Cambridge, MA) for the use of the PLKO.1-TRC cloning vector. The authors also thank the Mayo Clinic Advanced Genomics Technology Center for sequencing services and the Mayo Clinic Center for Translational Science Activities for statistical support.

Grant Support

This study was funded by NIH grants CA62164 and CA116964 (both to R.B. Diasio) and a grant from the Mayo Clinic Center for Individualized Medicine (S.M. Offer). Mayo Clinic Cancer Center shared resources used for this study were funded by a National Cancer Institute Cancer Center Support Grant 5P30 CA15083-37.

The costs of publication of this article were defrayed in part by the payment of page charges. This article must therefore be hereby marked *advertisement* in accordance with 18 U.S.C. Section 1734 solely to indicate this fact.

Received October 15, 2013; revised November 25, 2013; accepted January 2, 2014; published OnlineFirst January 8, 2014.

References

1. Toxicity of fluorouracil in patients with advanced colorectal cancer: effect of administration schedule and prognostic factors. Meta-Analysis Group In Cancer. J Clin Oncol 1998;16:3537–41.
2. Johnson MR, Diasio RB. Importance of dihydropyrimidine dehydrogenase (DPD) deficiency in patients exhibiting toxicity following treatment with 5-fluorouracil. Adv Enzyme Regul 2001;41:151–7.
3. Offer SM, Wegner NJ, Fossum C, Wang K, Diasio RB. Phenotypic profiling of DPYD variations relevant to 5-fluorouracil sensitivity using real-time cellular analysis and *in vitro* measurement of enzyme activity. Cancer Res 2013;73:1958–68.
4. Caudle KE, Thorn CF, Klein TE, Swen JJ, McLeod HL, Diasio RB, et al. Clinical pharmacogenetics implementation consortium guidelines for dihydropyrimidine dehydrogenase genotype and fluoropyrimidine dosing. Clin Pharmacol Ther 2013;94:640–5.
5. Yen JL, McLeod HL. Should DPD analysis be required prior to prescribing fluoropyrimidines? Eur J Cancer 2007;43:1011–6.
6. Salonga D, Danenberg KD, Johnson M, Metzger R, Groshen S, Tsao-Wei DD, et al. Colorectal tumors responding to 5-fluorouracil have low gene expression levels of dihydropyrimidine dehydrogenase, thymidylate synthase, and thymidine phosphorylase. Clin Cancer Res 2000;6:1322–7.
7. Ishikawa Y, Kubota T, Otani Y, Watanabe M, Teramoto T, Kumai K, et al. Thymidylate synthetase and dihydropyrimidine dehydrogenase levels in gastric cancer. Anticancer Res 1999;19:5635–40.
8. Huang CL, Yokomise H, Kobayashi S, Fukushima M, Hitomi S, Wada H. Intratumoral expression of thymidylate synthase and dihydropyrimidine dehydrogenase in non-small cell lung cancer patients treated with 5-FU-based chemotherapy. Int J Oncol 2000;17:47–54.
9. Kobayashi H, Koike T, Nakatsuka A, Kurita H, Sagara J, Taniguchi S, et al. Dihydropyrimidine dehydrogenase expression predicts survival outcome and chemosensitivity to 5-fluorouracil in patients with oral squamous cell carcinoma. Oral Oncol 2005;41:38–47.

Published OnlineFirst January 8, 2014; DOI: 10.1158/1535-7163.MCT-13-0878

10. Fernandez-Salguero P, Gonzalez FJ, Etienne MC, Milano G, Kimura S. Correlation between catalytic activity and protein content for the polymorphically expressed dihydropyrimidine dehydrogenase in human lymphocytes. Biochem Pharmacol 1995;50:1015–20.
11. Johnson MR, Wang K, Smith JB, Heslin MJ, Diasio RB. Quantitation of dihydropyrimidine dehydrogenase expression by real-time reverse transcription polymerase chain reaction. Anal Biochem 2000;278: 175–84.
12. Miyamoto S, Ochiai A, Boku N, Ohtsu A, Tahara M, Yoshida S, et al. Discrepancies between the gene expression, protein expression, and enzymatic activity of thymidylate synthase and dihydropyrimidine dehydrogenase in human gastrointestinal cancers and adjacent normal mucosa. Int J Oncol 2001;18:705–13.
13. Johnston SJ, Ridge SA, Cassidy J, McLeod HL. Regulation of dihydropyrimidine dehydrogenase in colorectal cancer. Clin Cancer Res 1999;5:2566–70.
14. Ezzeldin HH, Lee AM, Mattison LK, Diasio RB. Methylation of the DPYD promoter: an alternative mechanism for dihydropyrimidine dehydrogenase deficiency in cancer patients. Clin Cancer Res 2005;11:8699–705.
15. Noguchi T, Tanimoto K, Shimokuni T, Ukon K, Tsujimoto H, Fukushima M, et al. Aberrant methylation of DPYD promoter, DPYD expression, and cellular sensitivity to 5-fluorouracil in cancer cells. Clin Cancer Res 2004;10:7100–7.
16. Savva-Bordalo J, Ramalho-Carvalho J, Pinheiro M, Costa VL, Rodrigues A, Dias PC, et al. Promoter methylation and large intragenic rearrangements of DPYD are not implicated in severe toxicity to 5-fluorouracil-based chemotherapy in gastrointestinal cancer patients. BMC Cancer 2010;10:470.
17. Hirota T, Date Y, Nishibatake Y, Takane H, Fukuoka Y, Taniguchi Y, et al. Dihydropyrimidine dehydrogenase (DPD) expression is negatively regulated by certain microRNAs in human lung tissues. Lung Cancer 2012;77:16–23.
18. Moffat J, Grueneberg DA, Yang X, Kim SY, Kloepfer AM, Hinkle G, et al. A lentiviral RNAi library for human and mouse genes applied to an arrayed viral high-content screen. Cell 2006;124:1283–98.
19. Matsuda T, Cepko CL. Electroporation and RNA interference in the rodent retina *in vivo* and *in vitro*. Proc Natl Acad Sci U S A 2004;101: 16–22.
20. Saharia A, Guittat L, Crocker S, Lim A, Steffen M, Kulkarni S, et al. Flap endonuclease 1 contributes to telomere stability. Curr Biol 2008;18: 496–500.
21. Keene JD, Komisarow JM, Friedersdorf MB. RIP-Chip: the isolation and identification of mRNAs, microRNAs and protein components of ribonucleoprotein complexes from cell extracts. Nat Protoc 2006; 1:302–7.
22. Offer SM, Lee AM, Mattison LK, Fossum C, Wegner NJ, Diasio RB. A DPYD variant (Y186C) in individuals of African ancestry is associated with reduced DPD enzyme activity. Clin Pharmacol Ther 2013;94:158–66.
23. Purcell S, Neale B, Todd-Brown K, Thomas L, Ferreira MA, Bender D, et al. PLINK: a tool set for whole-genome association and population-based linkage analyses. Am J Hum Genet 2007;81:559–75.
24. Krek A, Grun D, Poy MN, Wolf R, Rosenberg L, Epstein EJ, et al. Combinatorial microRNA target predictions. Nat Genet 2005;37: 495–500.
25. Rehmsmeier M, Steffen P, Hochsmann M, Giegerich R. Fast and effective prediction of microRNA/target duplexes. RNA 2004;10: 1507–17.
26. Lorenz R, Bernhart SH, Höner Zu Siederdissen C, Tafer H, Flamm C, Stadler PF, et al. ViennaRNA Package 2.0. Algorithms Mol Biol 2011; 6:26.
27. The 1000 Genomes Browser. Hinxton, Cambridgeshire (UK): The European Bioinformatics Institute (EBI). (1000 Genomes release 13). [cited 2013 April 25]; Available from: http://browser.1000genomes.org/index.html
28. Zeng Y, Yi R, Cullen BR. Recognition and cleavage of primary microRNA precursors by the nuclear processing enzyme Drosha. EMBO J 2005;24:138–48.
29. Noratto GD, Jutooru I, Safe S, Angel-Morales G, Mertens-Talcott SU. The drug resistance suppression induced by curcuminoids in colon cancer SW-480 cells is mediated by reactive oxygen species-induced disruption of the microRNA-27a-ZBTB10-Sp axis. Mol Nutr Food Res 2013;57:1638–48.
30. Sreevalsan S, Safe S. The cannabinoid WIN 55,212-2 decreases specificity protein (Sp) transcription factors and the oncogenic cap protein eIF4E in colon cancer cells. Mol Cancer Ther 2013;12: 2483–93.
31. Chen Z, Ma T, Huang C, Zhang L, Lv X, Xu T, et al. MiR-27a modulates the MDR1/P-glycoprotein expression by inhibiting FZD7/beta-catenin pathway in hepatocellular carcinoma cells. Cell Signal 2013;25: 2693–701.
32. Oshikata A, Matsushita T, Ueoka R. Enhancement of drug efflux activity via MDR1 protein by spheroid culture of human hepatic cancer cells. J Biosci Bioeng 2011;111:590–3.
33. Thomson DW, Bracken CP, Goodall GJ. Experimental strategies for microRNA target identification. Nucleic Acids Res 2011;39: 6845–53.
34. Yang R, Schlehe B, Hemminki K, Sutter C, Bugert P, Wappenschmidt B, et al. A genetic variant in the pre-miR-27a oncogene is associated with a reduced familial breast cancer risk. Breast Cancer Res Treat 2010;121:693–702.
35. Kontorovich T, Levy A, Korostishevsky M, Nir U, Friedman E. Single nucleotide polymorphisms in miRNA binding sites and miRNA genes as breast/ovarian cancer risk modifiers in Jewish high-risk women. Int J Cancer 2010;127:589–97.
36. Zhang N, Huo Q, Wang X, Chen X, Long L, Jiang L, et al. A genetic variant in pre-miR-27a is associated with a reduced breast cancer risk in younger Chinese population. Gene 2013;529:125–30.
37. Sun Q, Gu H, Zeng Y, Xia Y, Wang Y, Jing Y, et al. Hsa-mir-27a genetic variant contributes to gastric cancer susceptibility through affecting miR-27a and target gene expression. Cancer Sci 2010; 101:2241–7.
38. Zhou Y, Du WD, Chen G, Ruan J, Xu S, Zhou FS, et al. Association analysis of genetic variants in microRNA networks and gastric cancer risk in a Chinese Han population. J Cancer Res Clin Oncol 2012; 138:939–45.
39. Hezova R, Kovarikova A, Bienertova-Vasku J, Sachlova M, Redova M, Vasku A, et al. Evaluation of SNPs in miR-196-a2, miR-27a and miR-146a as risk factors of colorectal cancer. World J Gastroenterol 2012;18:2827–31.

Published OnlineFirst January 8, 2014; DOI: 10.1158/1535-7163.MCT-13-0878

Molecular Cancer Therapeutics

microRNAs miR-27a and miR-27b Directly Regulate Liver Dihydropyrimidine Dehydrogenase Expression through Two Conserved Binding Sites

Steven M. Offer, Gabriel L. Butterfield, Calvin R. Jerde, et al.

Mol Cancer Ther 2014;13:742-751. Published OnlineFirst January 8, 2014.